Bowls, Balls and Sheets of Boric Acid Clusters: The Role of Pentagon and Hexagon Motifs

M. Elango, R. Parthasarathi, and V. Subramanian*

Chemical Laboratory, Central Leather Research Institute, Adyar, Chennai, India 600 020

N. Sathyamurthy*

Department of Chemistry, Indian Institute of Technology Kanpur, Kanpur, India 208 016

Received: June 22, 2005; In Final Form: August 3, 2005

Ab initio calculations suggest the possibility of forming boric acid clusters in the laboratory. The most stable form of the boric acid dimer contains two hydrogen bonds, similar to the carboxylic acid dimers. Though the trimer and the tetramer form extensions of this geometry, the pentamer prefers a bowl shape. Any addition of boric acid molecules to this geometry leads to bowl-shaped structures with the 15-mer forming a (3/4)-buckyball and the 20-mer a full-fledged buckyball. The hexamer, on the other hand, prefers to stay planar as a hexagon-centered rosette. Any further extension of this geometry leads to planar structures as long as a pentagon is not included.

Introduction

The discovery of fullerene by Kroto et al.[1] and carbon nanotube by Iijima[2] has kindled enormous research activity in the field of chemistry, physics, and biology to design and develop similar molecules. These new materials have potential applications in the fields of materials science, biotechnology, and medicine as nanoscale probes, sensors, and switches. The wealth of information available on the importance of hydrogen bonding in the structure and function of biological molecules is amazing! Inspired by the role of hydrogen bonding in the self-assembly of various molecules and molecular machines at the nano level in biology, several attempts have been made to design self-assembled molecular clusters using hydrogen-bonding interaction. The concept of buckyball-shaped water clusters as structural motifs has a long history in the form of clathrates.[3] Recently, ab initio calculations on clathrate-like water clusters with buckminsterfullerene as the guest species have been carried out by Ludwig and Appelhagen.[4] The hydrogen-bonded clusters of protonated water in various topologies have been investigated using experimental and theoretical methodologies.[5]

There have been several reports on the structure and properties of self-assembled organic and inorganic moieties. The literature is too vast to be reviewed here. The formation of boric acid-based nanometer- or micrometer-sized tubes, tips, and rods has been reported recently,[6] and their possible applications in submicron scale devices have also been explored. In this context, it is worth probing the structure and stability of boric acid (BA) clusters in various topologies. The equilibrium geometry of BA in its ground electronic state has C_{3h} point symmetry.[7] It has been found from the crystal structure of BA that it has a layered structure like graphite. Within a layer, each BA is hydrogen bonded to three other BAs.[8] The OH···O hydrogen bonding between the BAs stabilizes the layered structure.[9] Just as buckyballs and nanotubes are made from graphite sheets, one wonders if one could do the same with boric acid layers. Therefore, an ab initio electronic structure investigation of boric acid and its clusters was undertaken. Before the results could be published, Wang et al.[10] pointed out the possibility of self-curl and self-assembly of boric acid clusters using density functional theory with B3LYP parametrization and the 6-31G* basis set. They have also pointed out the tendency to form cage and cage-inside-cage structures by large clusters.[11] Therefore, in the present paper, we focus our attention on the structure of smaller clusters and the nature of their interaction. This is particularly important because different geometries arise at different stages of molecular cluster growth. For example, water clusters with 3−5 water molecules form rings. Only for the water hexamer do three-dimensional structures seem to become important. For still larger clusters, the tendency is to form structures consisting of stacked cubes and stacked pentagons. The much anticipated buckyball structure does not materialize for the water 20-mer![12] The protonated water clusters, on the other hand, tend to form chains initially and then form the cage for $(H_2O)_{21}H^+$.[5]

Computational Details

Geometries of various clusters of boric acid $(BA)_n$, $n = 1-20$, have been optimized without geometrical constraints at different levels of theory using the G98W suite of programs.[13] All of them are found to be stable relative to the separated monomers. The stabilization energies (SE) of all the clusters have been calculated using the supermolecule approach:

$$\mathrm{SE} = |E_{\mathrm{cluster}} - E_{\mathrm{monomers}}| \qquad (1)$$

and corrected for basis set superposition error (BSSE) following the procedure adopted by Boys and Bernardi.[14] Hartree−Fock (HF) and Møller−Plesset second-order perturbation (MP2) theoretic calculations using 6-31G* basis set for $(BA)_n$, $n = 2$ and 3, showed that the geometry optimization results were indistinguishable but the MP2 calculations yielded larger SEs. For optimal utilization of computational resources, therefore, only HF/6-31G* calculations were carried out for $4 \leq n \leq 20$.

* Authors for correspondence. V.S.: e-mail, subuchem@hotmail.com; tel, +91 44 24411630; fax, +91 44 24911589. N.S.: e-mail, nsath@iitk.ac.in; tel, +91 512 2597390/2597367; fax, +91 512 2597390.

10.1021/jp053382+ CCC: $30.25
Published on Web 09/07/2005

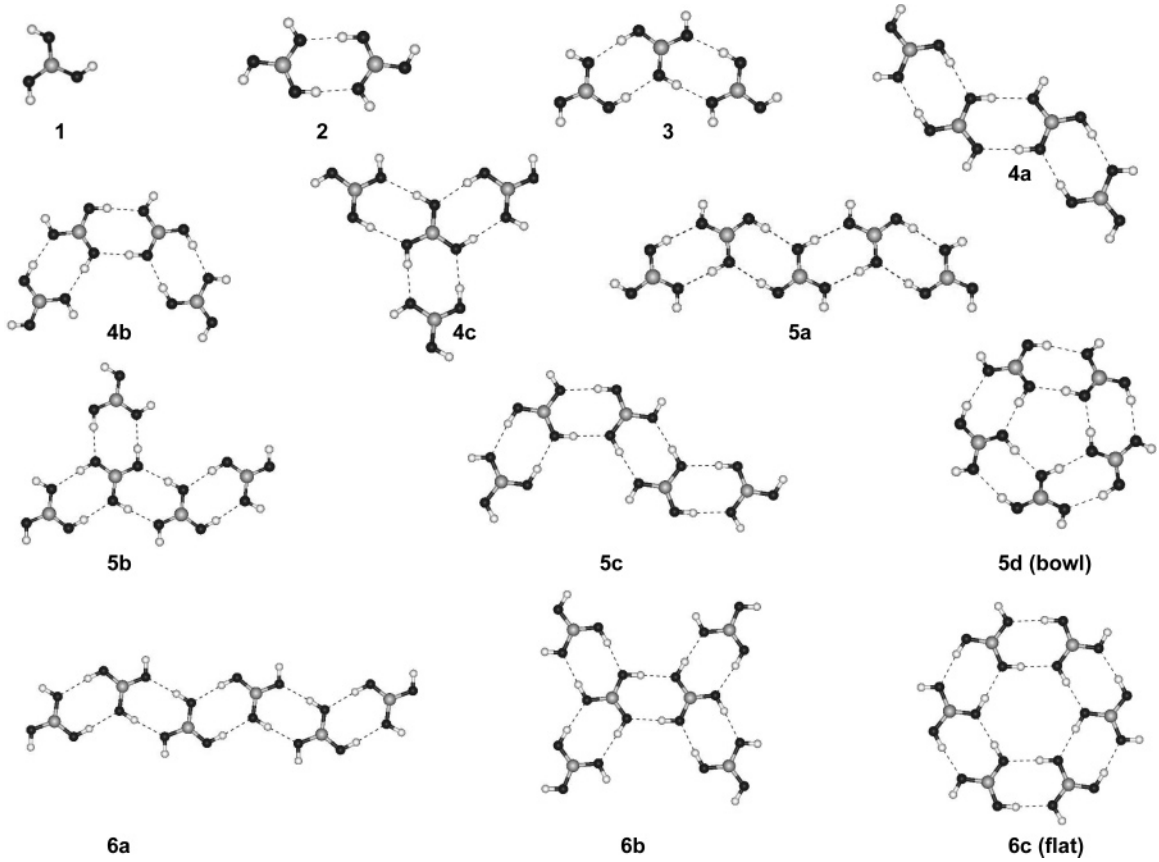

Figure 1. Optimized structure of $(BA)_n$ clusters where $n = 1-6$. The black spheres represent oxygen atoms, large gray spheres represent boron atoms, and smaller white spheres represent hydrogen atoms.

TABLE 1: Stabilization Energies (SE), Number of Hydrogen Bonds (N_{HB}) of All the Boric Acid $(BA)_n$ Clusters Obtained from HF/6-31G* Calculation (MP2 Energies in Brackets)

		stabilization energy (kcal/mol)			
n	N_{HB}	BSSE uncorrected	BSSE corrected	BSSE & ZPE corrected	BSSE corrected SE per BA (kcal/mol)
2	2	10.2 (14.4)	9.2 (11.7)	7.8	4.6 (5.9)
3	4	20.8 (29.6)	18.7 (23.9)	16.0	6.2 (8.0)
4 (**4a**)	6	32.1	28.5	24.4	7.1
4 (**4b**)	6	31.5	28.2	24.1	7.1
4 (**4c**)	6	31.7	28.3	24.2	7.1
5 (**5a**)	8	42.3	37.8	32.4	7.6
5 (**5b**)	8	42.2	37.7	32.3	7.5
5 (**5c**)	8	42.9	38.1	32.7	7.6
5 (**5d**) (bowl)	10	49.5	43.4	36.9	8.7
6 (**6a**) (linear)	10	52.9	47.2		7.9
6 (**6b**)	10	54.2	47.9		8.0
6 (**6c**) (planar)	12	64.6	57.2	49.2	9.5
6 (**6d**) (bowl)	12	60.7	53.2		8.8
8 (**8a**) (linear)	14	74.3	66.2		8.3
8 (**8b**) (bowl)	18	90.5	78.9	67.3	9.9
10 (linear)	18	95.6	85.3		8.5
10 (bowl)	24	121.0	104.9		10.5
12 (bowl)	30	152.0	131.0		10.9
15 (bowl)	40	203.0	174.6		11.7
20 (ball)	60	304.7	260.7		13.0

To ensure that the optimized geometries indeed corresponded to true minima in the energy space, vibrational frequencies were calculated for $(BA)_n$, $n = 1-8$. They were scaled by a factor of 0.8929 for comparison with the available experimental result for BA monomer. The theory of atoms-in-molecules (AIM)[15] has been used to characterize the hydrogen-bonding interaction using topological properties of electron density at the hydrogen bond critical points (HBCPs) using the AIM2000 package.[16] In addition, molecular electrostatic potential (MESP)[17] topography of various clusters have been generated using GaussianView 3.0 software package[18] and compared with that of C_{60}.

TABLE 2: Hydrogen Bonding Interaction Distances and Angles for $(BA)_n$ Clusters, Where $n = 2-6$ and 20 Obtained Using HF/6-31G* Calculation

n	type of H bonding	O−H distance (Å)	(O)H···O distance (Å)	O−H···O angle (deg)
1		0.946		
2		0.953	1.948	175.6
3		0.953	1.934	176.5
4		0.954	1.930	176.5
5	inner OH···O	0.957	1.853	166.6
	peripheral OH···O	0.952	2.063	165.2
6	inner OH···O	0.957	1.899	178.1
	peripheral OH···O	0.953	1.933	174.6
20		0.956	1.930	163.1

Results and Discussion

The equilibrium geometries of $(BA)_n$, $n = 1-6$, as obtained from HF/6-31G* calculations are presented in Figure 1. The optimized geometrical parameters of BA at HF/6-31G* level compare well with the experimental values. The calculated BO bond length and BOH bond angle are 1.358 Å and 112.5°, respectively, which are in close agreement with corresponding X-ray crystal structure values 1.361 Å and 114.0°. The calculated OH bond length is 0.946 Å. The stabilization energies computed, along with BSSE corrections and the number of hydrogen bonds (N_{HB}) are listed in Table 1 for all the clusters. For clusters up to $n = 8$, the zero point energy (ZPE) corrected SEs are also included in Table 1. The BA monomer in its ground

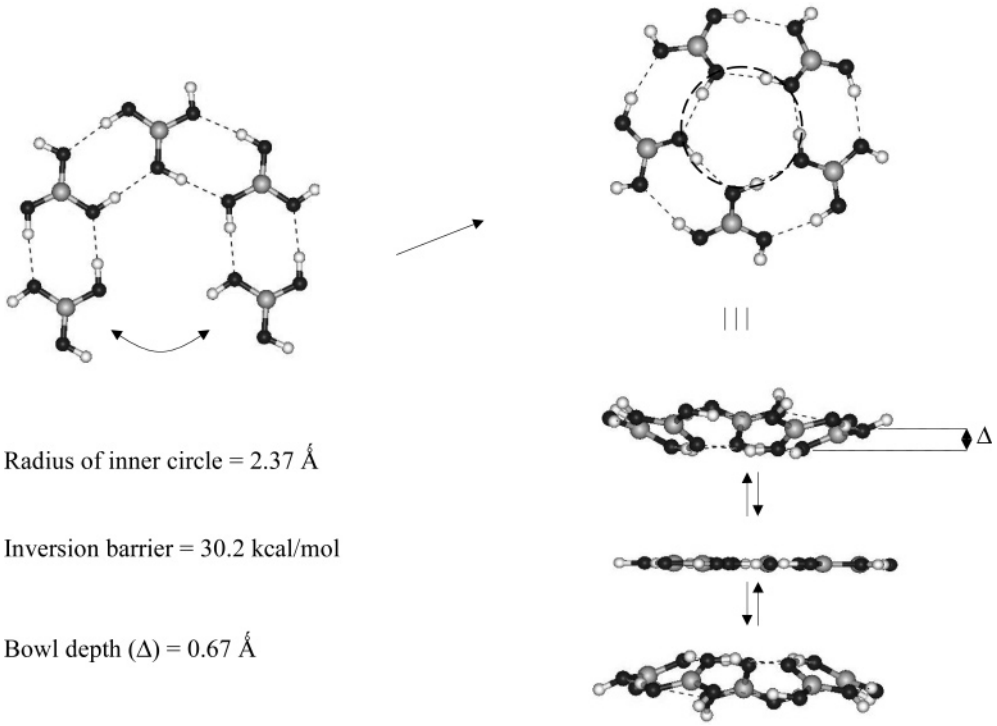

Figure 2. Structural features of the bowl-shaped boric acid pentamer **5d**, computed at the HF/6-31G* level. The bowl depth is calculated without considering the terminal hydrogen atoms.

electronic state is planar. In the dimer there are two identical OH···O interactions with the same set of geometrical parameters. Both the BA molecules act as hydrogen donors as well as acceptors. The BSSE corrected stabilization energy obtained for the dimer using HF and MP2 levels of theory is 9.2 and 11.7 kcal/mol, respectively. That makes the strength of each hydrogen bond 4.6 and 5.9 kcal/mol, comparable to that in water[12] and other such hydrogen-bonded species.

The hydrogen-bonded trimer is a planar structure in which the central BA is hydrogen bonded to two other BAs, one on either side. It is worth pointing out that one of the three oxygen atoms of the central boric acid molecule acts as a donor as well as an acceptor of a proton and hence participates in forming two hydrogen bonds. The HF calculation yields a stabilization energy of 18.7 kcal/mol (4.7 kcal/mol per hydrogen bond) and the same at the MP2 level is 23.9 kcal/mol. Therefore, it becomes clear that for quantitative predictions, HF/6-31G* calculations are inadequate. As a matter of fact, any quantitative prediction of the composition of boric acid in terms of the different clusters in the gas phase would require not only energy consideration but also entropy consideration. However, our primary interest in the present study is to compare the relative stabilities of different clusters and not their absolute numbers or composition.

There are at least three different structures possible for $(BA)_4$. It is possible to classify **4a** and **4b** as cis and trans tetramers. In **4c** the central BA is hydrogen bonded to three other BAs in a Y-shaped fashion. The difference between the stabilization energies for all the three tetramers is less than 1 kcal/mol, indicating easy interconversion between them.

Four different hydrogen-bonded structures are shown for the pentamer. While **5a**, **5b**, and **5c** are extensions of their tetrameric analogues, **5d** takes on the shape of a bowl as the closed loop cis extension of **4b**. It looks very similar to corannulene, the bowl-shaped precursor to fullerene-like topologies. It is important to emphasize that the stabilization energy of **5d** is more than that of the other linear pentamers. The bowl-shaped $(BA)_5$ with one hydrogen-bonded pentagon of oxygen atoms surrounded by five hydrogen-bonded hexagons of boron and oxygen atoms could form the basis for a boric acid "bucky ball". The fullerene-like topologies require a minimum of 12 pentagons and any number (n_{hex}) of hexagons to form a polyhedron of $2n_{hex} + 20$ vertexes. It is therefore expected that a fullerene-like topology would be obtained in boric acid clusters with 20 or more BAs self-assembled by hydrogen-bonding interaction.

Hydrogen-bonding geometries for the bowl-shaped pentamer are listed in Table 2. Clearly, there are two types of hydrogen-bonding distances, with the inner (O)H···O distance (1.85 Å) being considerably shorter than the outer (O)H···O (2.06 Å). All the inner hydrogen bonds are equivalent among themselves and the same is true of the outer hydrogen bonds. The inner pentagon has a radius of 2.37 Å, and the bowl has a depth of 0.67 Å. Understandably, the bowl can undergo inversion as illustrated in Figure 2. Investigations show the barrier for inversion to be ~30 kcal/mol. This also implies that the planar configuration for the pentamer is not stable; it is the transition state between the two bowls. Because boron has a valence of three and boric acid monomer is planar, the $(BA)_5$ bowl (depth 0.67 Å) is shallower than that of corannulene, which has a depth of 0.83 Å.[19] Although the bowl-to-bowl inversion barrier for $(BA)_5$ is less than that (36 kcal/mol) reported for corannulene,[20] it is large enough to give stability to $(BA)_5$-based structures.

The cyclic form (**6c**) of boric acid hexamer is found to be more stable than the other open and branched structures (**6a** and **6b**). Unlike the cyclic pentamer, the cyclic hexamer is planar, not bowl shaped! This is not surprising as the crystal structure of boric acid is made up of layers of hydrogen-bonded networks of hexagons.[9] To make sure that the planar $(BA)_6$ is the most stable, we have considered addition of a BA unit to the bowl-shaped $(BA)_5$ and found the bowl-based $(BA)_6$ is less stable by 4.2 kcal/mol. Additional optimized structures of pentagon- and hexagon-based $(BA)_n$ clusters, where $n = 7-10$, are listed in Figure 3, and they show clearly that the pentagon-

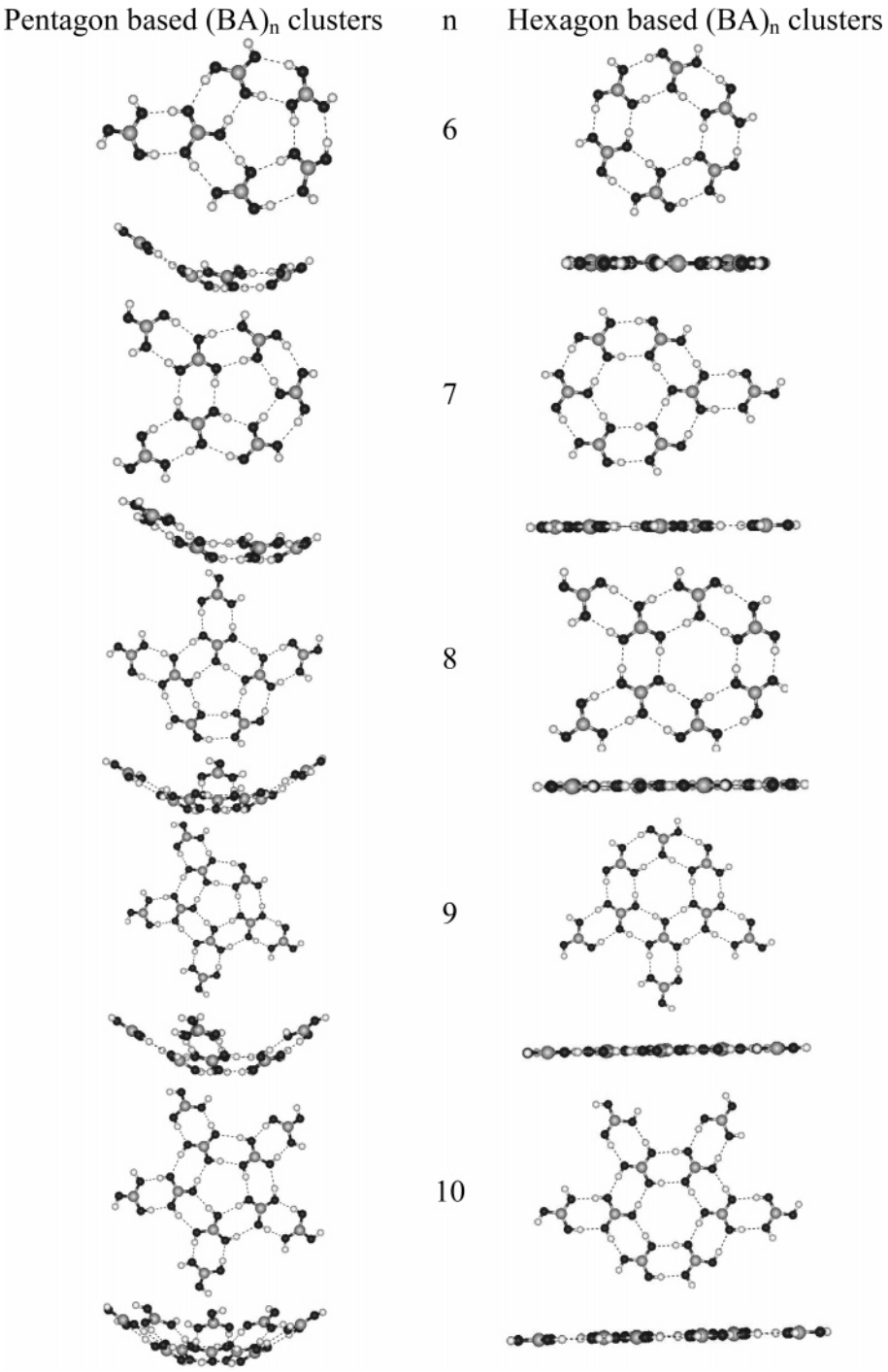

Figure 3. Optimized structures of pentagon- and hexagon-based $(BA)_n$ clusters, where $n = 6-10$. All the calculations were carried out at HF level of theory using the 6-31G* basis set. To clarify the bowl-shaped and flat structures, the side view is also shown in each case.

based structures are bowl shaped and the hexagon-based structures are flat. Therefore, energetically, it would be more favorable to build bowls and balls of BA clusters from $(BA)_5$ units and not $(BA)_6$!

Such a finding on the role of pentagons and hexagons in forming bowls and sheets is not completely new. It has been known in the case of carbon that the graphite sheet is hexagon based. To form bowls and balls of carbon, the pentagon motif is essential. But an identical situation in $(BA)_n$ clusters was not expected. The bonding in carbon clusters is covalent and largely rigid. The interaction between BA moieties in $(BA)_n$ clusters, on the other hand, is hydrogen bonding and is flexible to some extent.

Optimized geometries of larger clusters based on $(BA)_5$ are shown in Figure 4. Clearly, the 8-mer, 12-mer, and 15-mer are all bowl shaped, with the 15-mer approaching three-fourths of a buckyball. It is important to point out that the stabilization energy per BA moiety increases with increase in the size of the bowl. For small clusters, the hexagon-based flat structures are more stable than the pentagon-based bowl structures as illustrated in Figure 5a. However, as the bowls grow into balls, the stabilization energy continues to increase with increase in n, as illustrated in Figure 5b and as pointed out by Wang et al.[11] In contrast, the SE per BA for the hexagon-based structures remains constant for $n = 7-10$, as shown in Figure 5a.

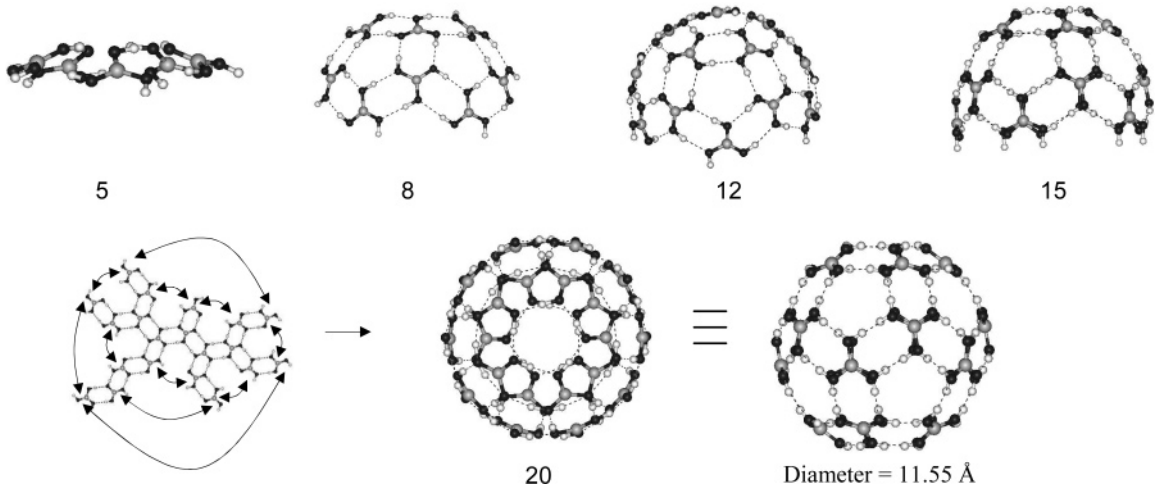

Figure 4. Optimized geometries of bowl-shaped structures and the boric acid ball obtained in this study. The initial geometry, which self-assembled to form buckyball upon optimization, is also provided.

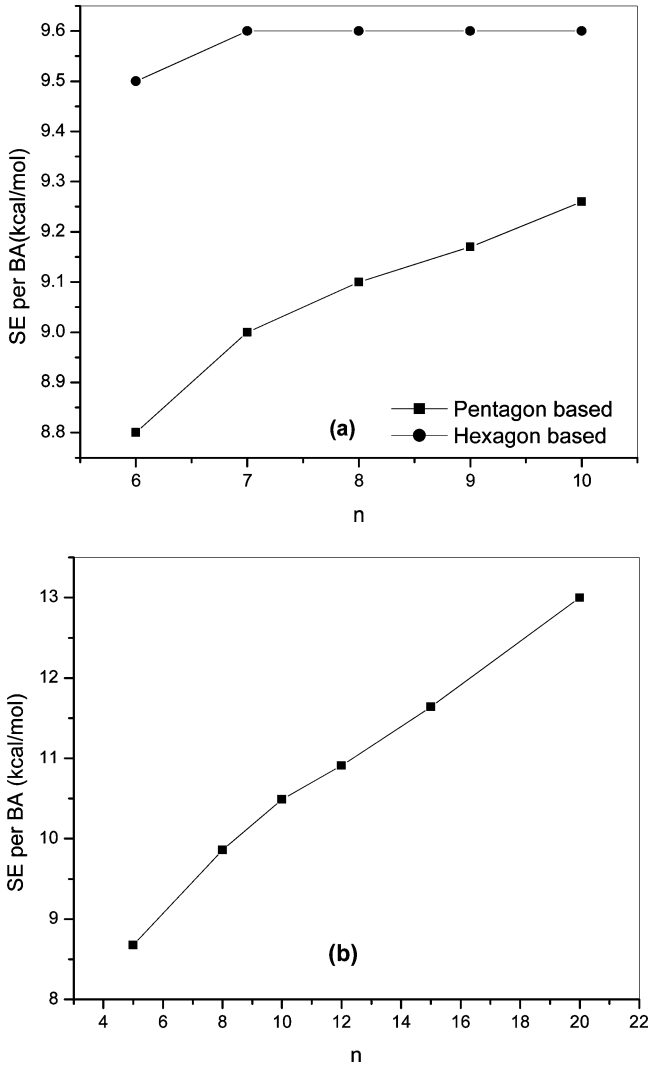

Figure 5. (a) The variation of stabilization energy (SE) per boric acid molecule in various pentagon- and hexagon-based $(BA)_n$ clusters, where $n = 6-10$, computed at the HF/6-31G* level. (b) Same as in (a) for bowl- and ball-shaped structures with $n = 5-20$.

Three-fourths-fullerene topology in $(BA)_n$ clusters is attained for $n = 15$. A close examination of the structure reveals the presence of one $(BA)_{10}$ belt concatenated to a $(BA)_5$ bowl with the help of a hydrogen-bonded network. It is interesting to note that in the belt-shaped $(BA)_{10}$, each BA molecule is hydrogen bonded to the neighboring BAs in a zigzag fashion. It is also observed that only $(BA)_n$ clusters with an even value of n can give rise to these belt-shaped clusters. The belt-shaped structure can be considered as a precursor for the boric acid nanotubes observed recently.[6]

With the addition of another $(BA)_5$ bowl to $(BA)_{15}$ described above, the structure would become a full-fledged fullerene-like boric acid ball! The optimized structure has got the same number of hexagons and pentagons as C_{80}. However, $(BA)_{20}$ is a perfect ball with 60 hydrogen bonds unlike C_{80}. The diameter of the boric acid ball as obtained from HF/6-31G* calculation is 11.55 Å, considerably larger than that (7.1 Å) for C_{60}. This is understandable as the edges of the pentagons and two out of the six edges of the hexagons of $(BA)_{20}$ are made up of long

TABLE 3: Electron Density and Laplacian of Electron Density at the Hydrogen-Bonding Critical Points for $(BA)_n$ Clusters Where $n = 2-6$ and 20 Using HF/6-31G* Calculation

n	type of H bonding	electron density (e/a_0^3)	Laplacian of electron density (e/a_0^5)
2		0.024	0.021
3		0.025	0.022
4		0.026	0.023
5	inner OH···O	0.030	0.027
	peripheral OH···O	0.019	0.017
6	inner OH···O	0.027	0.024
	peripheral OH···O	0.025	0.022
20		0.026	0.022

TABLE 4: Calculated Vibrational Frequencies of Various $(BA)_n$ Clusters at the HF/6-31G* Level, along with Computed Red Shifts in the O−H Stretching Mode

		scaled frequencies (cm^{-1})		red shift (cm^{-1})	
n	type of H bonding	ss	as	ss	as
1		3692 [3705][a]	3695 [3706][a]		
2		3572	3589	120	106
3		3540−3563	3576−3590	142−164	116−130
4		3513−3563	3537−3590	142−192	116−169
5	inner OH···O	3464	3503−3531	228	164−192
	peripheral OH···O	3593	3598−3607	99	88−97
6	inner OH···O	3476	3504−3535	216	160−191
	peripheral OH···O	3569	3577−3591	123	104−118

[a] The experimental values[7] are given in brackets. ss: symmetric stretch. as: asymmetric stretch.

Figure 6. AIM-derived molecular graphs of $(BA)_n$ clusters, where $n = 2$, 5, and 6 as obtained from HF/6-31G* calculation. Bond critical points are denoted by small red dots and the yellow dots represent ring critical points.

OH···O hydrogen bonds, in contrast to the short C−C bonds in fullerene.

The AIM theory has been used to characterize the hydrogen-bonding interactions in $(BA)_n$, $n = 2-6$, 20, and the resulting parameters are listed in Table 3. The values of electron density at the hydrogen bond critical points fall in the range 0.019−0.030 e/a_0^3. The Laplacian of the electron density at the CPs provide valuable information about the regions of electron concentration or depletion. The calculated values (0.017−0.027 e/a_0^5) of the Laplacian for the hydrogen bonds are all positive, indicating the depletion of electron density at the hydrogen-bonded CPs. Figure 6 gives the AIM topography for $(BA)_n$, $n = 2$, 5, and 6.

Symmetric and asymmetric O−H stretching frequencies for BA and its clusters up to $n = 6$ as computed by HF/6-31G* method and scaled by a factor of 0.8929 are reported in Table 4. The computed values of 3692 and 3695 cm^{-1} for BA monomer compare very well with the experimental values of 3705 and 3706 cm^{-1}. The corresponding values of 3572 and 3589 cm^{-1} for the dimer show clearly a red shift of 120 and 106 cm^{-1}, respectively, thus indicating hydrogen bond formation. The computed red shifts in the range 116−192 cm^{-1} for the trimer and the tetramer reiterate the characteristic of hydrogen bonding.[21] Due to slightly different types of hydrogen bonding in the inner and outer peripheries of the pentamer as well as the hexamer, the red shifts are also different. Hydrogen bonding in the inner periphery results in a larger red shift than that in the outer periphery for both $(BA)_5$ and $(BA)_6$.

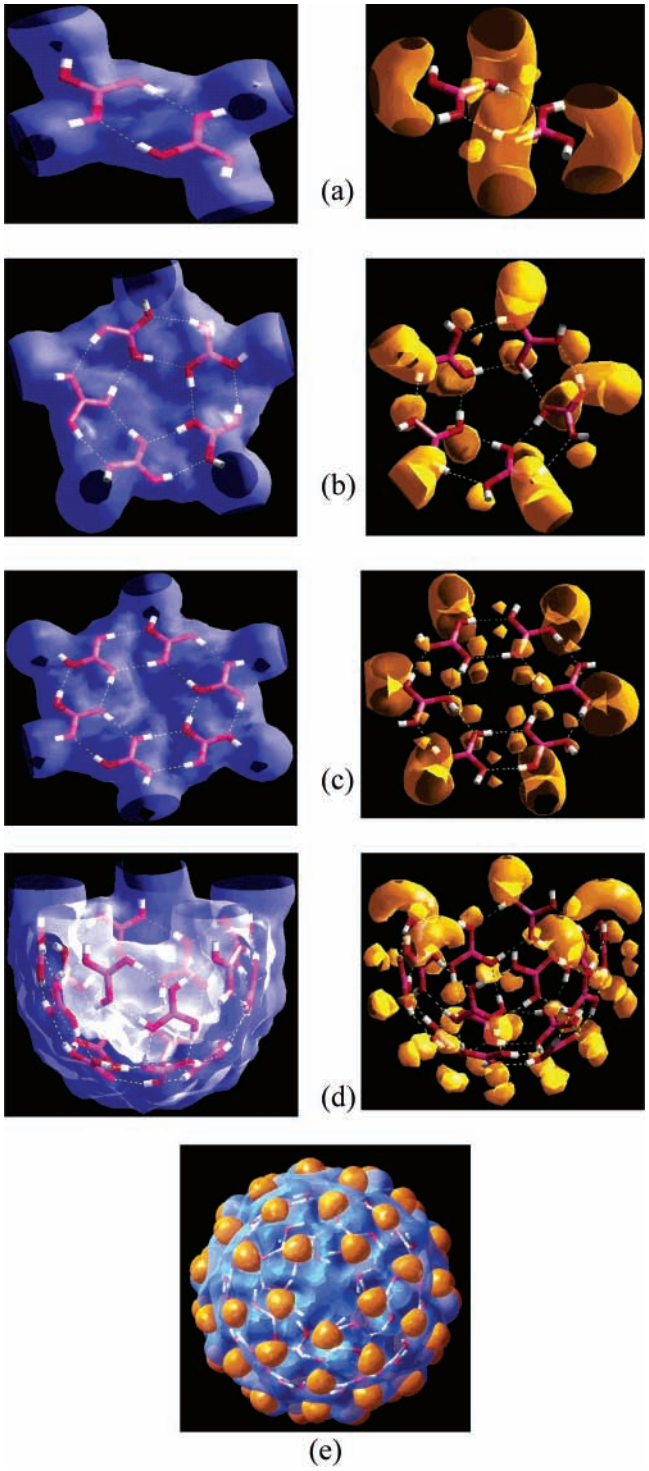

Figure 7. MESP features of $(BA)_n$ clusters for (a) $n = 2$, (b) $n = 5$, (c) $n = 6$, (d) $n = 15$, and (e) $n = 20$. Blue represents the +0.01 au isosurface, and orange represents the −0.01 au isosurface.

Because the molecular electrostatic potential (MESP) map is a valuable tool to understand the reactivity of various molecules, it has been computed for $(BA)_n$, $n = 2$, 5, 6, 15, and 20, and the −0.01 and 0.01 au isosurfaces are illustrated in Figure 7. The 0.01 au isosurface reveals clearly that the positive MESP features occur on both sides of the molecular plane. It can be seen from the negative-valued MESP isosurface of the dimer that the crescent shape indicating the MESP minimum occurs at the position of the lone pairs of the free oxygen atom.

It can also be seen from Figure 7 that the size of the crescent-shaped isosurface near the hydrogen-bonded oxygen is less than that of the non-hydrogen-bonded oxygen. These regions provide possible anchoring sites for further hydrogen-bonding interactions. It is interesting to look at the MESP features for the bowl-shaped $(BA)_{15}$. Positive electrostatic potential can be seen inside as well as outside the bowl, whereas the negative-valued MESP is found only outside the bowl, as shown in Figure 7d. A combination of both negative- and positive-valued MESP isosurfaces for the $(BA)_{20}$ ball is shown in Figure 7e. It is to be noted that the negative-valued MESP features are seen only at the outside of the ball whereas the positive MESP values are observed both inside and outside of the ball. This is very similar to what is observed for C_{60}. Inside the cage it is positive everywhere and outside there are regions of negative and positive potentials.

Despite the fact that water molecule is bent and that it can act as a donor as well as an acceptor of hydrogen bonds, the hollow cage (buckyball) structure does not seem to be the most stable geometry for $(H_2O)_{20}$.[12] Water clusters tend to form cuboid and pentagonoid structures. Therefore, it is particularly interesting that boric acid clusters can assume the shapes of bowls and balls by putting together $(BA)_5$ and $(BA)_{10}$ moieties.

Summary and Conclusion

Ab initio quantum chemical calculations suggest that boric acid molecules can self-assemble into various topologies such as bowls and balls as long as they are built around $(BA)_5$ moieties. The planar hexamer-based structures, on the other hand, continue to be planar as long as a pentagon is not introduced. The planar hexamer, for example, is more stable than the pentagon-based hexamer by 4.2 kcal/mol.

Acknowledgment. This study was supported in part by a grant from the Council of Scientific and Industrial Research, New Delhi, India. M.E., R. P., and V. S. are grateful to Dr. T. Ramasami for his continued support.

References and Notes

(1) Kroto, H. W.; Heath, J. R.; O'Brien, S. C.; Curl, R. F.; Smalley, R. E. *Nature* **1985**, *318*, 162.
(2) Iijima, S. *Nature* **1991**, *354*, 56.
(3) Pauling, L. *The Nature of the Chemical Bond*, 3rd ed.; Cornell University Press: Ithaca, NY, 1960; p 469.
(4) Ludwig, R.; Appelhagen, A. *Angew. Chem., Int. Ed.* **2005**, *44*, 811.
(5) Miyazaki, M.; Fujii, A.; Ebata, T.; Mikami, N. *Science* **2004**, *304*, 1134. Shin, J.-W.; Hammer, N. L.; Diken, E. G.; Johnson, M. A.; Walters, R. S.; Jaeger, T. D.; Duncan, M. A.; Christie, R. A.; Jordan, K. D. *Science* **2004**, *304*, 1137.
(6) Li, Y.; Ruoff, R. S.; Chang, R. P. H. *Chem. Mater*. **2003**, *15*, 3276.
(7) Andrews, L.; Burkholder, T. R. *J. Chem. Phys.* **1992**, *97*, 7203; Zaki, K.; Pouchan, C. *Chem. Phys. Lett.* **1995**, *236*, 184.
(8) Zachariasen, W. H. *Z. Kristallogr*. **1934**, *88*, 150; *Acta Crystallogr*. **1954**, *7*, 305.
(9) Zapol, P.; Curtiss, L. A.; Erdemir, A. *J. Chem. Phys.* **2000**, *113*, 3338.
(10) Wang, W.; Zhang, Y.; Huang, K. *Chem. Phys. Lett*. **2005**, *405*, 425.
(11) Wang, W.; Zhang, Y.; Huang, K. *J. Phys. Chem. B* **2005**, *109*, 8562.
(12) Maheshwary, S.; Patel, N.; Sathyamurthy, N.; Kulkarni, A. D.; Gadre, S. R. *J. Phys. Chem. A* **2001**, *105*, 10525.
(13) Frisch, M. J.; et al.*Gaussian 98*, revision A.7; Gaussian, Inc.: Pittsburgh, PA, 1998.
(14) Boys, S. F.; Bernardi, F. *Mol. Phys.* **1970**, *19*, 553.
(15) Bader, R. F. W. *Atoms in Molecules: A Quantum Theory;* Clarendon Press: Oxford, U.K., 1990.
(16) Biegler-Konig, F.; Schonbohm, J.; Derdau, R.; Bayles, D.; Bader, R. F. W. *AIM 2000*, version 1; Bielefeld, Germany, 2000.
(17) Gadre, S. R.; Shirsat, R. N. *Electrostatics of Atoms and Molecules*; Universities Press: Hyderabad, 2000.
(18) *GaussianView 3.0*; Gaussian Inc.: Pittsburgh, PA, 2003.
(19) Seiders, T. J.; Baldridge, K. K.; Grube, G. H.; Siegel, J. S. *J. Am. Chem. Soc.* **2001**, *123*, 517.
(20) Dinadayalane, T. C.; Deepa, S.; Sastry, G. N. *Tetrahedron Lett*. **2003**, *44*, 4527.
(21) Jeffrey, G. A. *An Introduction to Hydrogen Bonding*; Oxford University Press: Oxford, NY, 1997.